Desalination and Water Treatment
www.deswater.com
doi: 10.5004/dwt.2023.29891

309 (2023) 255–261
October

Cellulose acetate/nano-zinc oxide bio-composites: the functional and anti-bacterial characteristics

Salah F. Abdellah Ali[a,b,*], Karam S. El-Nasser[a], Ibrahim O. Althobaiti[a,*]

[a]*Department of Chemistry, College of Science and Arts, Jouf University, Gurayat 77217, Saudi Arabia, Tel.: +966535083033; emails: sfali@ju.edu.sa (S.F. Abdellah Ali), ioalthobaiti@ju.edu.sa (I.O. Althobaiti)*
[b]*Materials Science Department, Institute of Graduate Studies and Research, Alexandria University, Egypt*

Received 27 June 2023; Accepted 27 July 2023

ABSTRACT

In this research article, the investigations of how nano-zinc oxide (N-ZnO) could be changed the functional and antimicrobial features of cellulose acetate (CA) films were established. As a result, three forms of CA films comprising 0.5%, 1.0%, and 2.0% N-ZnO have been assembled. Following that, the physicochemical and barrier properties were assessed. Further, the anti-bacterial activities of prepared nanocomposite films towards *Escherichia coli* have been investigated using Fourier-transform infrared spectroscopy (FTIR). The obtained results demonstrated that 2.0% N-ZnO had the greatest impact on physicochemical and barrier properties. The FTIR spectra revealed that all N-ZnO concentration interactions were physical, with no chemical reactions between the nanoparticles and CA framework. The incorporation of N-ZnO improved the humidity level, water absorption, and uptake capability of CA films, which are essential factors in packaging manufacturing. The anti-bacterial effect of 2.0% N-ZnO formulation exhibited a stronger anti-bacterial impact compared to the remaining formulations. Subsequently, N-ZnO improved the overall properties of CA films and the most satisfactory concentration for utilizing N-ZnO in CA-based nanocomposite films was 2% N-ZnO.

Keywords: Anti-bacterial activity; Nano-zinc oxide; Nanotechnology; Cellulose acetate (CA)

1. Introduction

Synthetic polymers offer important thermal and mechanical characteristics, as well as a cheap cost and ease of production. As a result, these polymers are commonly employed in the packaging sectors [1]. However, the amount of plastic trash is increasing, and it will likely harm our planet. The packaged food industries are attempting to limit the use of plastics in favour of natural and sustainable biodegradable polymers derived from various resources [2]. For packaging uses, some biopolymers have been incorporated [3]. Bioplastics are made from renewable agricultural resources and biomass feedstock, making them environmentally friendly and long-lasting [4]. Natural plastic is formed in a fluid state, so it can be readily moulded and does not require a lot of energy. This contrasts with the ordinary plastic, which is often held as granules and requires a tremendous amount of energy to form by normal ways of manufacturing [5]. Among the biopolymer matrices used in the creation of bioplastics, cellulose is thought to be the raw ingredient. Cellulose is the most abundant component in all plant materials [6]. To increase the quality of bioplastics, cellulose is transformed into cellulose acetate [7]. Biodegradable polymers based on cellulose acetate were investigated, and the resultant material disintegrated in soil or water within few years. However, the material may also be recycled or destroyed without leaving a trace. There has been researching on the key qualities of cellulose acetate such as mechanical strength, impact resistance, transparency, di-electric properties, and fabrication [8]. The use of nanotechnology is one of the most successful ways to overcome some of the issues and improve the performance of various natural polymers. Different organic and inorganic nano-fillers are

* Corresponding authors.

Presented at the European Desalination Society Conference on Desalination for the Environment: Clean Water and Energy, Limassol, Cyprus, 22–26 May 2023

employed in nanotechnology to increase the functional and anti-bacterial features [9]. Nano-zinc oxide (N-ZnO) has a distinctive morphology and structure, as well as considerable impacts of anti-microbial action towards a broad spectrum of micro-organisms [10]. The Food and Drug Administration (FDA) approved N-ZnO as a safe food ingredient and it has a favourable impact on the environment. Zinc is required for physiological activity and mankind's health, and every individual needs 10^{-2} g of zinc every day [11]. Many researches have been undertaken on the influence of N-ZnO on the characteristics of nanocomposite films and have confirmed the beneficial effects of these nanoparticles on the functional and anti-bacterial activities of the generated films [12]. Researchers have also investigated the influence of the morphology and the size of nanoparticles on the antimicrobial performances of N-ZnO, and the results suggested that both the morphology and size of the studied nanomaterials have a major effect on various microorganisms [13]. Few number of publications have been undertaken on the use of N-ZnO in various matrixes to investigate its impact on the operational and antimicrobial activities of biopolymer-based matrix [14]. The objective of this study is to investigate the influence of N-ZnO on different characteristics and anti-bacterial activities of cellulose acetate matrix [15].

2. Materials and methods

2.1. Materials

Cellulose acetate (CA) has been sold from Acros Organics Co. N-ZnO has been sold from Sigma Chemical Co. The Immunology and Microbiology Department, Faculty of Medicine, Al-Azhar University graciously provided the references pathogens, *Escherichia coli* (gram-negative), and *Staphylococcus aureus* MRSA (gram-positive).

2.2. CA and N-ZnO nanocomposite film fabrication

N-ZnO was added to water at concentrations of 0.5%, 1.0%, and 2.0% w/w (related to CA weight), as shown in Table 1. These concentration ranges were chosen using the criteria proposed [16]. A hot plate at 70°C was then used to heat the solutions for 1 h. They are then shaken for 24 h without heat to create uniform solutions. Under ultrasonic conditions (50°C, 1 h), the obtained mixtures become homogeneous. Glycerol was utilized as a plasticizing agent at 40% w/w (based on dry matter). The CA dispersion was heated and stirred on a hot plate at 90°C for 1 h. The temperature was reduced to 40°C. The control film was made in the same way, but with no N-ZnO added. To form a film, 90 g of the homogeneous solution were placed onto moulding plates measuring 15 × 15 cm^2. CA films were dried at 40°C and 50% relative moisture for 24 h under controlled conditions. The dried CA specimens were taken away from the plates and put in a desiccator until testing [17].

Table 1
Different compositions of CA/N-ZnO films

Specimen No.	Specimen code	CA %	N-ZnO %
1	S0	100	0
2	S1	99.5	0.5
3	S2	99	1.0
4	S3	98	2.0

2.3. Characterization of CA films

2.3.1. Estimation of humidity content, water solubility, and water uptake capability

The content of humidity of the bio-nanocomposite films has been determined employing the protocol mentioned. The films' capacity to absorb water and their water solubility was assessed employing the procedures specified [18–20].

2.3.2. Oxygen and water vapor permeability assessment

Employing ASTM method E96/E96M-16 (ASTM, 2016), the water vapor permeability of prepared films has been assessed. In conclusion, the film has been subjected to 100% *moisture* for 2-d, and the level of permeability has been assessed at 25°C by weighing per 2 h. Utilizing ASTM standardized procedure D3985-17 (ASTM, 2017), the films' oxygen permeability has been evaluated.

2.3.3. Fourier-transform infrared spectroscopy

The chemical interaction was evaluated utilizing Fourier-transform infrared spectroscopy. Films with di-mentions of 1 and 20 cm on KBr tablets were placed inside the Fourier-transform infrared (FTIR) spectrophotometer cell. The infrared spectrum was recorded with an accuracy of 4 cm^{-1} and in the scope of 400–4,000 cm^{-1}.

2.3.4. Anti-bacterial evaluation

The anti-bacterial activities were evaluated towards gram-negative and gram-positive strains, *Escherichia coli* and *Staphylococcus aureus* MRSA. The strains have been first activated in Nutrient Broth (NB, Conda Lab, Spain) culture medium for 24 h under shaking conditions, then 50 L was inoculated in NB after serial dilution and the colony-forming units (CFU)/mL of the investigated strains have been determined. As a result, once we have determined the inoculum concentration, we adjust it to 10^6/mL. To determine the resistance ratios of the tested strains, the sensitivity of *Staphylococcus aureus* MRSA and *Escherichia coli* against Cephredem and Ciprofloxacin was determined. The anti-bacterial activities of the tested compounds were initially assessed using the agar well diffusion technique with Mueller Hinton Agar at a concentration of 20 g/mL. When compared to standard anti-bacterial drugs, the ability of each targeted compound to prevent bacterial growth was measured using the inhibition zone diameter (mm) [21]. Following that, the compounds' minimum inhibitory concentration was determined in comparison to a standard drug using the broth micro dilution method. To prepare the stock solution, 10 mg of each compound and reference drug were dissolved in 1 mL of sterilized deionized water. Ten successive dilutions with concentrations ten times higher than the final solution of the synthesized

compounds were prepared [22]. The dilutions were then diluted to 1:5 in Mueller Hinton Broth (MHB), and 100 l aliquots have been consecutively distributed into the microdilution plates to achieve concentrations ranging from 5 to 160 g/mL. Each compound was incubated for 24 h at 37°C with the tested bacterial strain. The control growth samples were MHB mixed with deionized water [23]. To calculate the growth curves of the diversified bacterial pathogens, the absorbance of the suspension at 630 nm has been used. The percentage of inhibition of growth and cell viability in untreated and treated cells observed by turbidimetry has been calculated utilizing the equation [24].

$$A = \frac{B}{A} \times 100$$

where B and A are the absorbances of the treated and untreated specimens, respectively.

The lowest concentration of each compound that yielded a lower number of bacterial cells when compared to untreated samples was used to calculate the minimum inhibitory concentration.

3. Results and discussion

3.1. Impact of N-ZnO on the humidity level of CA films

One of the issues limiting film use is *moisture* sensitivity. Fig. 1 illustrates the humidity level of films bearing varying dosages of N-ZnO. Incorporating varying concentrations of N-ZnO and raising respective concentrations, as depicted in Fig. 1, diminished the humidity levels of the generated film as compared to the reference film. The *moisture* content of the films was reduced to the most in the films comprising 2% N-ZnO. The reference film had a *moisture* content of 10.60%, while the 2% film had a *moisture* content of 6.70%. When contrasted to the control, the coherent structure having strong cohesion and lower hydrophilicity of N-ZnO than the CA-based polymer matrix resulted in diminished humidity of CA films comprising 2% N-ZnO. The incorporation of N-ZnO and TiO_2 into bio-nanocomposite films was also reported [25].

3.2. Impact of N-ZnO on the water-solubility of CA films

The water solubility of CA films incorporating N-ZnO with various concentrations is displayed in Fig. 2. According to the findings, the standard exhibited the maximum water solubility (28.76%), and the solubility of the nanocomposite films was dramatically decreased by the addition of N-ZnO and raising respective concentrations in CA films. Once the N-ZnO concentration was increased, the solubility dropped to 19.84%. The decrease in solubility of N-ZnO-containing biopolymer-based films is most likely due to interactions between N-ZnO and CA in the film matrix. According to research, as the number of nanoparticles in biofilms increases, stronger hydrogen bonds originate between N-ZnO and the polymer framework. Consequently, free water particles are unable to penetrate as deeply as they can with composite films alone. In studies, N-ZnO has been added to lower the water solubility of films derived from biopolymers [26,27]. These investigations demonstrated that the incorporation of N-ZnO increased the formation of hydrogen bonding amongst both N-ZnO and film and thus deactivating free water particles and inhibiting their interaction with the nanocomposite matrix. The solubility of films comprising pectin/alginate was shown to be reduced by the addition of N-ZnO [26,27].

3.3. Impact of N-ZnO on water uptake capacity of CA films

The water uptake capacity of N-ZnO bio-nanocomposite films is displayed in Fig. 3. The standard CA matrix exhibited the maximum amount (2.27 g/g dried weight), and the water uptake capacity was significantly reduced by adding various N-ZnO and raising their doses in the matrix. The impact of N-ZnO on water uptake capacity was more noticeable at 2% N-ZnO. The films containing 2% N-ZnO (1.12 g/g dried weight) had the lowest water uptake capacity. This reduction could be attributed to the CA biopolymer matrix nanostructure's empty spaces being filled. Nanostructures could be reacted with CA's hydroxyl moieties, reducing the number of sites available for the attachment of water to CA and lowering the water uptake capacity of the matrix. Furthermore, it has been found that the addition of N-ZnO reduced the water uptake capacity of film-based sago starch and bovine gelatin. The effect of N-ZnO on the water uptake capacity of sodium caseinate-based membranes was also illustrated [28].

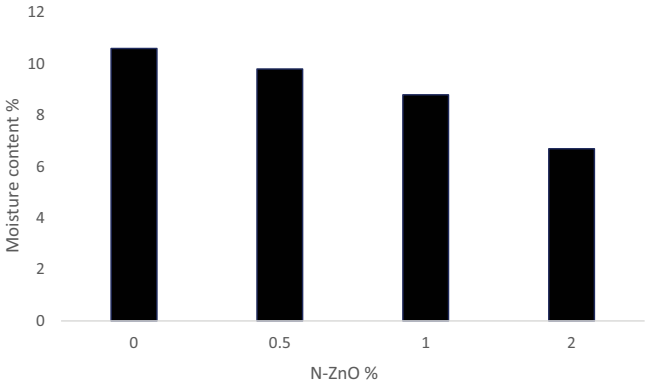

Fig. 1. Effect of N-ZnO on the *moisture* content of CA films.

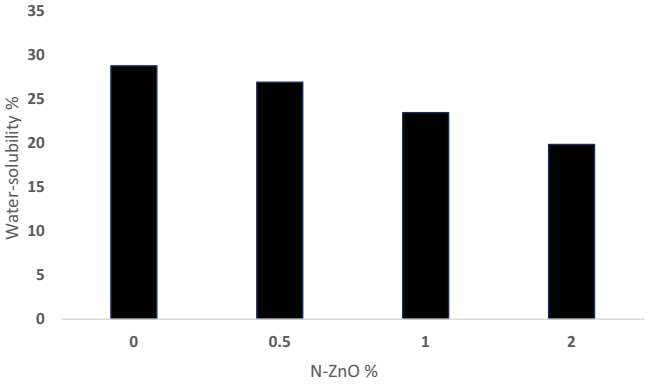

Fig. 2. Effect of N-ZnO on the water solubility of CA films.

3.4. Impact of N-ZnO on barrier- properties of CA films

Figs. 4 and 5 display the oxygen and water steam permeabilities of nanocomposite membranes containing various N-ZnO. The control had the best results (6.28×10^{-10} g/m·s·Pa) and (287.30 cm^3 m/s) (m^2-d). The oxygen and water steam permeability of CA membranes was remarkably reduced by increasing the concentrations of N-ZnO in the membranes. The smallest amounts of permeability were (2.52×10^{-10} g/m·s·Pa) and (191.34 cm^3·m/(m^2-d)) in films containing 2% of N-ZnO. The diminution in the layer thickness of CA-based nano-composite films comprising various levels of N-ZnO could be ascribed mainly to the aspect that, in comparison to CA polymer merely, the existence of such nanomaterials inside the biopolymer matrix makes molecule movement more difficult. The incorporation of bio-nanocomposite might lessen the relative *moisture* transference since the speedy transfer of water steam represents the major drawback of biopolymer-based films. Generally, the improvement of bio-nanocomposite film barrier characteristics is caused by the establishment of sense and coherent frameworks. The inclusion of nanomaterials was found to dramatically diminish the water steam and oxygen permeabilities of biopolymer-based films [29].

3.5. Impact of N-ZnO on the FTIR spectroscopy of CA

Certain infrared (IR) radiation frequencies are absorbed by the various bonds and functional motifs in the chemical structures. FTIR spectroscopy is a useful tool for studying structural modifications in chemical composites. The FTIR of CA-based nanomaterial membranes comprising various forms of N-ZnO at levels of 0%, 0.5%, 1.0%, and 2.0% is shown in Fig. 6. Pure CA has a specific absorption peak at around 3,285 cm^{-1} attributed to vibrational frequency of the OH group. This OH groups are responsible for the formation of complicated tensile vibrations accompanied by the free intramolecular and intermolecular hydroxyl groups existing in CA's natural biopolymer framework. Further, the C–O bonds existing in C–O–H and C–O–C of the glucose motifs are related to the wavenumber 1,108 and 1,028 cm^{-1}. Also, the vibration of CA's C–O–C ring is associated with absorption bands 921 and 850 cm^{-1}. Peaks in the 1,200–1,500 cm^{-1} range have been assigned to C–H and O–H bonds. It is obvious that the introduction of N-ZnO could not lead to the creation of any novel functional groups. As a result, the interaction established between the N-ZnO and CA-polymer molecules is a physical type. Incorporating N-ZnO into sodium caseinate membranes caused no remarkable modifications in the polymer matrix's structure and no new bonds to form [30–33].

3.6. Impact of N-ZnO on the anti-bacterial activities of CA films towards Escherichia coli

E. coli is among the most widespread harmful bacteria found in food products. It is transmitted orally, and it should never be found in food or food products. As a result, *E. coli* counts are used as a food safety and hygiene indicator bacterium. Increasing the concentrations of different N-ZnO forms in bio-composite films increased their anti-bacterial activity. In general, various mechanisms for metal nanoparticle antimicrobial action have been proposed, the utmost substantial of which are catalytic reduction and oxidation activities that influences DNA, enzyme active sites, and ribosome activities. These functions interfere with bacterial metabolism. There are several suggested actions for the anti-microbial activities of metal nanomaterials including the induction of active oxygen species for example, hydrogen peroxide, hydroxyl radicals, superoxide, and cell wall

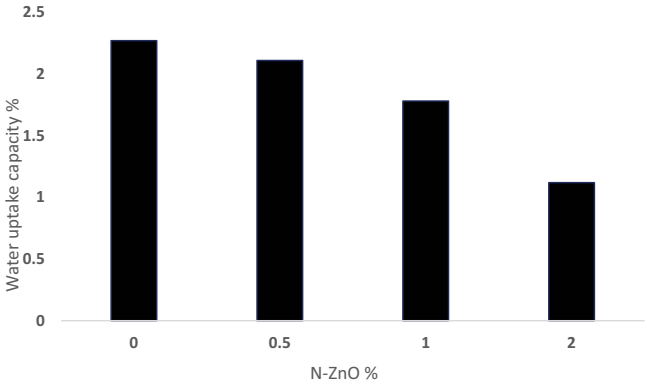

Fig. 3. Effect of N-ZnO on water uptake capacity of CA films.

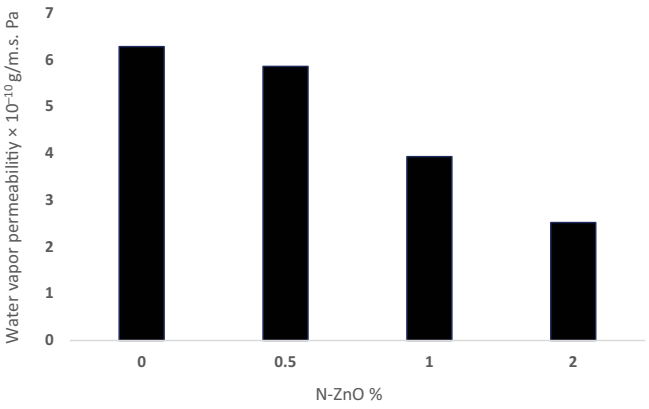

Fig. 4. Water vapor permeability of CA films.

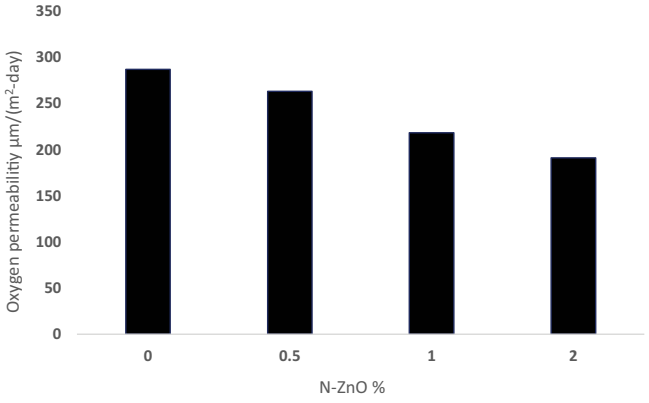

Fig. 5. Oxygen permeability of CA films.

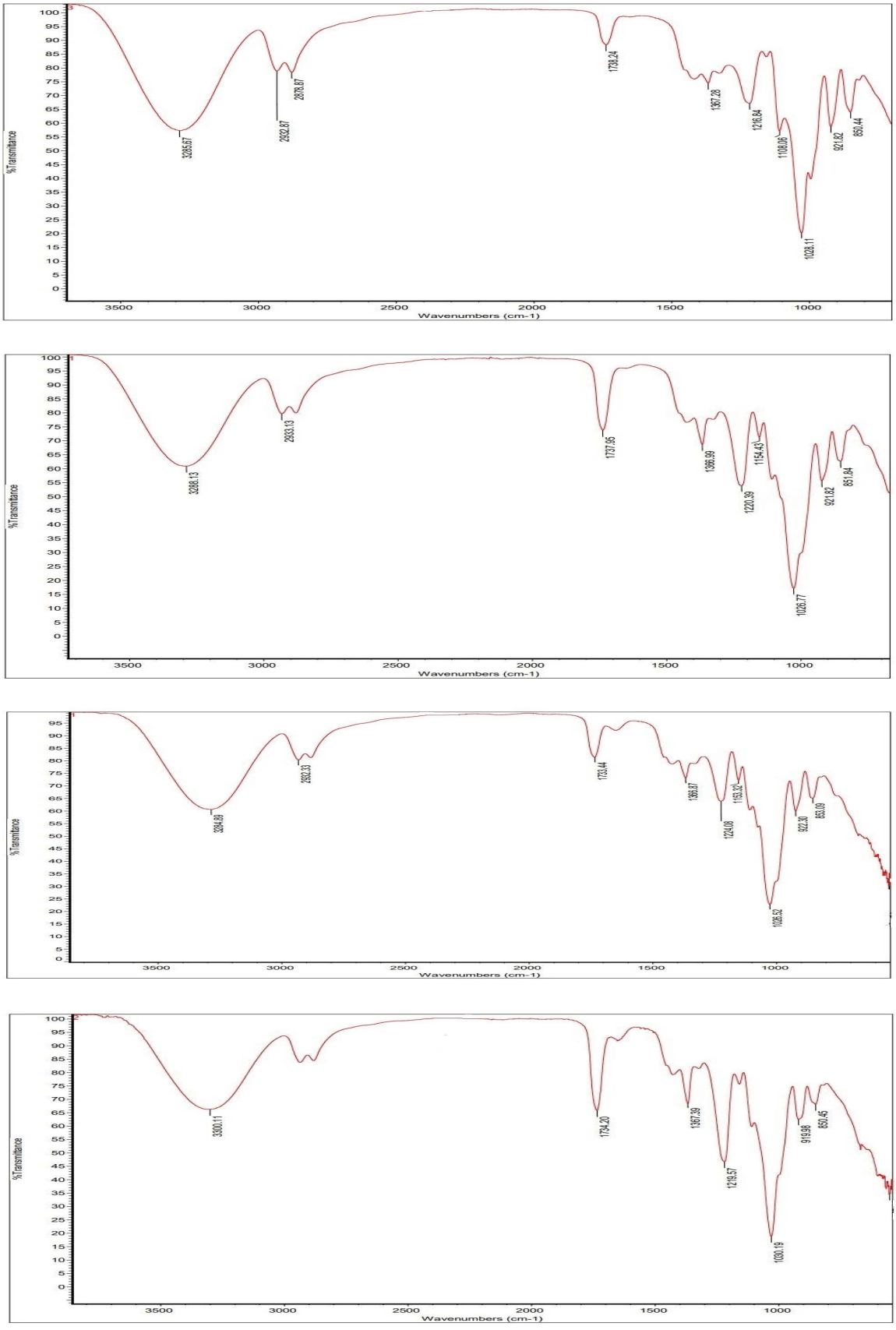

Fig. 6. FTIR of CA films containing 0%, 0.5%, 1.0% and 2.0% of N-ZnO.

Table 2
Anti-bacterial activity (diffusion method)

Specimen	Code	Inhibition zone (mm)	
		Escherichia coli (gram-negative)	*Staphylococcus aureus* MRSA (gram-positive)
1	S0	7	4
2	S1	11	5
3	S2	9	4
4	S3	12	7
Vancomycin		10	6
Cephradine		7	ND

Vancomycin and Cephradine were used as positive controls, ND: not determined.

Table 3
Minimum inhibitory concentration of the targeted compounds

Sample No.	Sample code	Minimum inhibitory concentration (μg/mL)	
		Escherichia coli (gram-negative)	*Staphylococcus aureus* MRSA (gram-positive)
1	S0	10	40
2	S1	20	10
3	S2	10	20
4	S3	5	5
Vancomycin		5	25
Cephradine		80	ND

damage. In the presence of bacterium cells, N-ZnO's charges interact with the bacteria's negative charges. Owing to the created electrostatic forces, the bacteria's cell membrane is destroyed, allowing the release of intracellular materials [34–36]. As shown in Table 2, bacterial pathogens were clearly resistant to the classic anti-bacterial agent Cephradine, whereas Vancomycin had a weak anti-bacterial ability against *Staphylococcus aureus*. With varying ratios, the targeted compounds had a strong inhibitory effect. Furthermore, targeted compounds exhibited high bactericidal susceptibility with lower minimum inhibitory concentration values (Table 3), which were found to be equivalent to or greater than the standard anti-bacterial agent Vancomycin [37–39].

Screening of the targeted compounds was preliminary take place at a concentration of 20 μg/mL using agar well diffusion method.

4. Conclusion

This research investigated the impacts of N-ZnO on the anti-bacterial, chemical, and physical properties of CA membranes. The outcomes showed that introducing various formats of N-ZnO and escalating their concentrations in nanocomposite films enhanced their chemical, physical, and anti-bacterial activities. The obtained nano-composite CA films possessed acceptable oxygen and water vapor permeability properties, besides significant anti-bacterial activity towards E. coli. Further, N-ZnO has the greatest impact on the functional and anti-bacterial activities of CA-based membranes at 2% concentration. Overall, this study found that ZnO nanomaterials have remarkable impacts on the performance of CA biopolymers.

References

[1] S.F. Abdellah Ali, Mechanical and thermal properties of promising polymer composites for food packaging applications, IOP Conf. Ser.: Mater. Sci. Eng., 137 (2016) 012035, doi: 10.1088/1757-899X/137/1/012035.
[2] A.M. Sharaf, E. Syala, A.A. Ezzat, S.F.A. Ali, E. El-Rafey, Natural fiber reinforced unsaturated polyester resin filled with bio-based calcium carbonate: preparation and examination, Fibers Polym., 23 (2022) 1366–1377.
[3] M. Akbariazam, M. Ahmadi, N. Javadian, A.M. Nafchi, Fabrication and characterization of soluble soybean polysaccharide and nanorod-rich ZnO bionanocomposite, Int. J. Biol. Macromol., 89 (2016) 369–375.
[4] K.M. Abd El-Rahman, S.F. Abdellah Ali, A.I. Khalil, S. Kandil, Influence of poly(butylene succinate) and calcium carbonate nanoparticles on the biodegradability of high density-polyethylene nanocomposites, J. Polym. Res., 27 (2020) 231, doi: 10.1007/s10965-020-02217-y.
[5] E. El-Rafey, W.M. Walid, E. Syala, A.A. Ezzat, S.F. Abdellah Ali, A study on the physical, mechanical, thermal properties and soil biodegradation of HDPE blended with PBS/HDPE-g-MA, Polym. Bull., 79 (2022) 2383–2409.
[6] H. Babapour, H. Jalali, A.M. Nafchi, The synergistic effects of zinc oxide nanoparticles and fennel essential oil on physicochemical, mechanical, and antibacterial properties of potato starch films, Food Sci. Nutr., 9 (2021) 3893–3905.
[7] S.F. Abdellah Ali, I.O. Althobaiti, E. El-Rafey, E.S. Gad, Wooden polymer composites of poly(vinyl chloride), olive pits flour, and precipitated bio-calcium carbonate, ACS Omega, 6 (2021) 23924–23933.
[8] E. Arezoo, E. Mohammadreza, M. Maryam, M.N. Abdorreza, The synergistic effects of cinnamon essential oil and nano TiO_2 on antimicrobial and functional properties of sago starch films, Int. J. Biol. Macromol., 157 (2020) 743–751.
[9] S.F. Abdellah Ali, Biodegradation properties of poly-ε-caprolactone, starch and cellulose acetate butyrate composites, J. Polym. Environ., 22 (2014) 359–364.
[10] S. Fawzi, A. Ali, Performance of cellulose acetate propionate in polycaprolactone and starch composites: biodegradation and water resistance properties, Biointerface Res. Appl. Chem., 10 (2020) 5382–5386.
[11] S.F. Abdellah Ali, M. El Batouti, M. Abdelhamed, E. El-Rafey, Formulation and characterization of new ternary stable composites: polyvinyl chloride-wood flour-calcium carbonate of promising physicochemical properties, J. Mater. Res. Technol., 9 (2020) 12840–12854.
[12] A. Emamifar, M. Kadivar, M. Shahedi, S. Soleimanian-Zad, Evaluation of nanocomposite packaging containing Ag and ZnO on shelf life of fresh orange juice, Innovative Food Sci. Emerg. Technol., 11 (2010) 742–748.
[13] J.E. Bruna, A. Peñaloza, A. Guarda, F. Rodríguez, M.J. Galotto, Development of $MtCu^{2+}$/LDPE nanocomposites with antimicrobial activity for potential use in food packaging, Appl. Clay Sci., 58 (2012) 79–87.
[14] M. Chaisawang, M. Suphantharika, Pasting and rheological properties of native and anionic tapioca starches as modified by guar gum and xanthan gum, Food Hydrocolloids, 20 (2006) 641–649.
[15] S. Saedi, M. Shokri, J.T. Kim, G.H. Shin, Semi-transparent regenerated cellulose/ZnONP nanocomposite film as a potential antimicrobial food packaging material, J. Food Eng., 307 (2021) 110665, doi: 10.1016/j.jfoodeng.2021.110665.
[16] M.M. Marvizadeh, N. Oladzadabbasabadi, A.M. Nafchi, M. Jokar, Preparation and characterization of bionanocomposite film based on tapioca starch/bovine gelatin/nanorod zinc oxide, Int. J. Biol. Macromol., 99 (2017) 1–7.

[17] S. Ekramian, H. Abbaspour, B. Roudi, L. Amjad, A.M. Nafchi, An experimental study on characteristics of sago starch film treated with methanol extract from *Artemisia sieberi* Besser, J. Food Meas. Charact., 15 (2021) 3298–3306.
[18] S. Ekramian, H. Abbaspour, B. Roudi, L. Amjad, A.M. Nafchi, Influence of *Nigella sativa* L. extract on physico–mechanical and antimicrobial properties of sago starch film, J. Polym. Environ., 29 (2021) 201–208.
[19] M. Maizura, A. Fazilah, M.H. Norziah, A.A. Karim, Antibacterial activity and mechanical properties of partially hydrolyzed sago starch-alginate edible film containing lemongrass oil, J. Food Sci., 72 (2017) 324–330.
[20] S. Kiatkamjornwong, W. Chomsaksakul, M. Sonsuk, Radiation modification of water absorption of cassava starch by acrylic acid/acrylamide, Radiat. Phys. Chem., 59 (2000) 413–427.
[21] Y.-l. Lv, F.-s. Zhang, J. Chen, J.-l. Cui, Y.-m. Xing, X.-d. Li, S.-x. Guo, Diversity and antimicrobial activity of endophytic fungi associated with the alpine plant *Saussurea involucrata*, Biol. Pharm. Bull., 33 (2010) 1300–1306.
[22] M. Mallique Qader, A.A. Hamed, S. Soldatou, M. Abdelraof, M.E. Elawady, A.S.I. Hassane, L. Belbahri, R. Ebel, M.E. Rateb, Antimicrobial and antibiofilm activities of the fungal metabolites isolated from the marine endophytes *Epicoccum nigrum* M13 and *Alternaria alternata* 13A, Mar. Drugs, 19 (2021) 232, doi: 10.3390/md19040232.
[23] M.A. El-Bendary, M.E. Moharam, M. Abdelraof, M.A. Allam, A.M. Roshdy, M.N.F. Shaheen, E.M. Elmahdy, G.M. Elkomy, Multi-bioactive silver nanoparticles synthesized using mosquitocidal Bacilli and their characterization, Arch. Microbiol., 202 (2020) 63–75.
[24] M.A. El-Bendary, M. Abdelraof, M.E. Moharam, E.M. Elmahdy, M.A. Allam, Potential of silver nanoparticles synthesized using low active mosquitocidal *Lysinibacillus sphaericus* as novel antimicrobial agents, Prep. Biochem. Biotechnol., 51 (2021) 926–935.
[25] A.M. Nafchi, A.K. Alias, S. Mahmud, M. Robal, Antimicrobial, rheological, and physicochemical properties of sago starch films filled with nanorod-rich zinc oxide, J. Food Eng., 113 (2012) 511–519.
[26] S. Teymourpour, A.M. Nafchi, F. Nahidi, Functional, thermal, and antimicrobial properties of soluble soybean polysaccharide biocomposites reinforced by nano TiO_2, Carbohydr. Polym., 134 (2015) 726–731.
[27] S. Tunç, O. Duman, Preparation and characterization of biodegradable methyl cellulose/montmorillonite nanocomposite films, Appl. Clay Sci., 48 (2010) 414–424.
[28] M. Alizadeh-Sani, E.M. Kia, Z. Ghasempour, A. Ehsani, Preparation of active nanocomposite film consisting of sodium caseinate, ZnO nanoparticles and rosemary essential oil for food packaging applications, J. Polym. Environ., 29 (2020) 588–598.
[29] T.M.P. Ngo, T.M.Q. Dang, T.X. Tran, P. Rachtanapun, Effects of zinc oxide nanoparticles on the properties of pectin/alginate edible films, Int. J. Polym. Sci., 2018 (2018) 5645797, doi: 10.1155/2018/5645797.
[30] S.F. Abdellah Ali, L.A. William, E.A. Fadl, Cellulose acetate, cellulose acetate propionate and cellulose acetate butyrate membranes for water desalination applications, Cellulose, 27 (2020) 9525–9543.
[31] M.F. Rosa, E.S. Medeiros, J.A. Malmonge, K.S. Gregorski, D.F. Wood, L.H.C. Mattoso, G. Glenn, W.J. Orts, S.H. Imam, Cellulose nanowhiskers from coconut husk fibers: effect of preparation conditions on their thermal and morphological behavior, Carbohydr. Polym., 81 (2010) 83–92.
[32] Y. Xiao, Y. Liu, S. Kang, K. Wang, H. Xu, Development and evaluation of soy protein isolate-based antibacterial nanocomposite films containing cellulose nanocrystals and zinc oxide nanoparticles, Food Hydrocolloids, 106 (2020) 105898, doi: 10.1016/j.foodhyd.2020.105898.
[33] Z. Moslehi, A.M. Nafchi, M. Moslehi, S. Jafarzadeh, Aflatoxin, microbial contamination, sensory attributes, and morphological analysis of pistachio nut coated with methylcellulose, Food Sci. Nutr., 9 (2021) 2576–2584.
[34] C.M.O. Müller, J.B. Laurindo, F. Yamashita, Effect of nanoclay incorporation method on mechanical and water vapor barrier properties of starch-based films, Ind. Crops Prod., 33 (2011) 605–610.
[35] A.M. Nafchi, A.K. Alias, Mechanical, barrier, physicochemical, and heat seal properties of starch films filled with nanoparticles, J. Nano Res., 25 (2013) 90–100.
[36] B. Ramalingam, T. Parandhaman, S.K. Das, Antibacterial effects of biosynthesized silver nanoparticles on surface ultrastructure and nanomechanical properties of gram-negative bacteria viz. *Escherichia coli* and *Pseudomonas aeruginosa*, ACS Appl. Mater. Interfaces, 8 (2016) 4963–4976.
[37] S.H. Othman, N.A. Majid, I.S.M.A. Tawakkal, R.K. Basha, N. Nordin, R.A. Shapi'i, Tapioca starch films reinforced with microcrystalline cellulose for potential food packaging application, Food Sci. Technol., 39 (2019) 605–612.
[38] N. Pariona, F. Paraguay-Delgado, S. Basurto-Cereceda, J.E. Morales-Mendoza, L.A. Hermida-Montero, A.I. Mtz-Enriquez, Shape-dependent antifungal activity of ZnO particles against phytopathogenic fungi, Appl. Nanosci., 10 (2020) 435–443.
[39] M.A. Raza, Z. Kanwal, A. Rauf, A.N. Sabri, S. Riaz, S. Naseem, Size- and shape-dependent antibacterial studies of silver nanoparticles synthesized by wet chemical routes, Nanomaterials, 6 (2016) 74, doi: 10.3390/nano6040074.